frontiers in Molecular Neuroscience

ORIGINAL RESEARCH
published: 06 September 2021
doi: 10.3389/fnmol.2021.663598

Pharmacological Rescue of the Brain Cortex Phenotype of *Tbx1* Mouse Mutants: Significance for 22q11.2 Deletion Syndrome

Ilaria Favicchia[1†], Gemma Flore[2†], Sara Cioffi[2], Gabriella Lania[2], Antonio Baldini[2,3] and Elizabeth Illingworth[1]*

[1] Department of Chemistry and Biology, "Adolfo Zambelli", University of Salerno, Fisciano, Italy, [2] Institute of Genetics and Biophysics "Adriano Buzzati-Traverso", CNR, Naples, Italy, [3] Department of Molecular Medicine and Medical Biotechnologies, University of Naples, Federico II, Naples, Italy

OPEN ACCESS

Edited by:
Arnau Hervera Abad, Institute for Bioengineering of Catalonia (IBEC), Spain

Reviewed by:
Jens Randel Nyengaard, Aarhus University, Denmark
M. Albert Basson, King's College London, United Kingdom

***Correspondence:**
Elizabeth Illingworth
eillingworth@unisa.it

[†] *These authors have contributed equally to this work*

Specialty section:
This article was submitted to Neuroplasticity and Development, a section of the journal Frontiers in Molecular Neuroscience

Received: *03 February 2021*
Accepted: *05 August 2021*
Published: *06 September 2021*

Citation:
Favicchia I, Flore G, Cioffi S, Lania G, Baldini A and Illingworth E (2021) Pharmacological Rescue of the Brain Cortex Phenotype of Tbx1 Mouse Mutants: Significance for 22q11.2 Deletion Syndrome. Front. Mol. Neurosci. 14:663598. doi: 10.3389/fnmol.2021.663598

Objectives: *Tbx1* mutant mice are a widely used model of 22q11.2 deletion syndrome (22q11.2DS) because they manifest a broad spectrum of physical and behavioral abnormalities that is similar to that found in 22q11.2DS patients. In *Tbx1* mutants, brain abnormalities include changes in cortical cytoarchitecture, hypothesized to be caused by the precocious differentiation of cortical progenitors. The objectives of this research are to identify drugs that have efficacy against the brain phenotype, and through a phenotypic rescue approach, gain insights into the pathogenetic mechanisms underlying *Tbx1* haploinsufficiency.

Experimental Approach: *Disease model*: *Tbx1* heterozygous and homozygous embryos. We tested the ability of two FDA-approved drugs, the LSD1 inhibitor Tranylcypromine and Vitamin B12, to rescue the *Tbx1* mutant cortical phenotype. Both drugs have proven efficacy against the cardiovascular phenotype, albeit at a much reduced level compared to the rescue achieved in the brain.

Methods: *In situ* hybridization and immunostaining of histological brain sections using a subset of molecular markers that label specific cortical regions or cell types. Appropriate quantification and statistical analysis of gene and protein expression were applied to identify cortical abnormalities and to determine the level of phenotypic rescue achieved.

Results: Cortical abnormalities observed in *Tbx1* mutant embryos were fully rescued by both drugs. Intriguingly, rescue was obtained with both drugs in *Tbx1* homozygous mutants, indicating that they function through mechanisms that do not depend upon *Tbx1* function. This was particularly surprising for Vitamin B12, which was identified through its ability to increase *Tbx1* gene expression.

Conclusion: To our knowledge, this is only the second example of drugs to be identified that ameliorate phenotypes caused by the mutation of a single gene from the 22q11.2 homologous region of the mouse genome. This one drug-one gene approach might be important because there is evidence that the brain phenotype in 22q11.2DS

patients is multigenic in origin, unlike the physical phenotypes, which are overwhelmingly attributable to *Tbx1* haploinsufficiency. Therefore, effective treatments will likely involve the use of multiple drugs that are targeted to the function of specific genes within the deleted region.

Keywords: *TBX1*, vitamin B12, pharmacological action, DiGeorge syndrome, Tranylcypromine

INTRODUCTION

Brain-related phenotypes, including intellectual disability and psychiatric disorders, are a major concern for the clinical management and quality of life of patients affected by 22q11.2 deletion syndrome (22q11.2DS). Several of the many genes heterozygously deleted in patients have been suggested to contribute to this group of phenotypes, based on data obtained in animal models. However, *TBX1*, the major candidate gene for the phenotypic findings linked to development of the embryonic pharynx, has been found to be mutated in patients with a 22q11.2DS-like phenotype that includes neurobehavioral anomalies. For example, *TBX1* mutation has been found in a patient with Asperger syndrome (Paylor et al., 2006) and in association with developmental delay (Torres-Juan et al., 2007; Ogata et al., 2014) and attention deficits (Haddad et al., 2019). Therefore, *TBX1* should be regarded as a major candidate for at least some of the brain-related clinical presentations in 22q11.2DS patients.

Mouse models have been instrumental not only for identifying the role of *Tbx1* in the disease, but also for determining its role in mouse behavior and brain development (Paylor and Lindsay, 2006; Paylor et al., 2006; Prasad et al., 2008; Flore et al., 2017; Motahari et al., 2019). *Tbx1* mutant mouse embryos have a complex brain cortex phenotype (Flore et al., 2017). Most interestingly, the heterozygous phenotype is almost as severe as the homozygous phenotype, indicating a high sensitivity of the brain cortex to *Tbx1* dosage. An additional peculiarity of Tbx1 function in the embryonic mouse brain is that it is mesoderm-dependent, thus mediated by an extracellular signal. This is also the case for several other phenotypes associated with the haploinsufficiency or loss of this gene (Zhang et al., 2005; Fagman et al., 2007; Xu et al., 2007; Braunstein et al., 2009; Calmont et al., 2009; Lania et al., 2009). In addition, recently, the mouse models have been used for testing experimental strategies for rescuing the cardiovascular phenotype, opening the way to targeted pre-clinical studies. The rescue of phenotypes caused by deficiency of *Tbx1*, which encodes a transcription factor, presents special challenges because of the potential number and variety of target genes. Nevertheless, research has identified a number of targeted strategies that have been successful in ameliorating the cardiovascular phenotype (Vitelli et al., 2010; Caprio and Baldini, 2014; Fulcoli et al., 2016; Lania et al., 2016; Racedo et al., 2017). However, the brain cortex phenotype has never been tested. Given the importance of the brain-related phenotype associated with 22q11.2DS, and because of the potential opportunity for clinical application, we tested two rescuing strategies in mice, selected on the basis of their potential clinical applicability. Results showed that the Lsd1/2 inhibitor Tranylcypromine (TCP) and Vitamin B12 (B12) prevent brain cortex abnormalities in *Tbx1* mutants.

MATERIALS AND METHODS

Mouse Lines and *in vivo* Drug Treatments

Mouse studies were performed according to current regulations under the animal protocol 257/2015-PR approved by the Italian Ministry of Health. $Tbx1^{lacz/+}$ (Lindsay et al., 2001) mice are maintained on a C57BL/6N background, $Tbx1^{+/\Delta E5}$ (Xu et al., 2004). Genotyping was performed as in the original reports. Administration of vitamin B12 (cyanocobalamin Sigma-Aldrich, V2876) was performed by intraperitoneal (i.p.) injection of pregnant female mice daily from E7.5 to E11.5 with 20 mg Kg^{-1} body weight of B12 dissolved in PBS. Control mice were injected with the same volume of PBS. Administration of TCP was performed as described for vitamin B12, using 10 mg Kg^{-1} body weight of TCP (Sigma-Aldrich, p8511-G) dissolved in sterile 0.9% w/v NaCl solution. Control mice were injected with the same volume of sterile 0.9% w/v NaCl solution. Developmental staging was established considering the morning of a visible vaginal plug as stage E0.5.

Phenotype Analysis

Pregnant females were sacrificed at E13.5. Phenotype evaluations were performed blind to the genotype.

(a) *In situ* hybridization on mouse embryo brain sections.

Cryosections: E13.5 brains were fixed in 4% PFA/1x PBS at 4°C overnight, washed in 1x PBS and incubated for 12 h in serial dilutions of sucrose/1x PBS (10, 20, 30% sucrose) at 4°C. Brains were then incubated for 2 h at 4°C in 50:50 v/v 30% sucrose in 1x PBS/OCT prior to embedding in OCT. Twenty micron coronal sections were cut along the rostral–caudal brain axis on a cryostat and were post-fixed in 4% PFA at RT for 10 min prior to immunostaining, except for immunofluorescence (IF). Alternatively, specimens were stored at -80°C. For *in situ* hybridization (ISH), antisense RNA probes were labeled using a DIG-RNA labeling kit (Roche). The probes used were: *Pax6*, *Tis21* and *NeuroD2*; DIG-labeled probes were hybridized to cryosections following published methods (Hirsch et al., 1998).

(b) Immunofluorescence and immunohistochemistry on mouse embryo brain sections.

Immunofluorescence (IF) was performed using the following primary antibodies: Mouse monoclonal anti-human KI67 antibody, 1:200 (BD Pharmingen, #556003) and rabbit polyclonal anti-phosphohistone 3 (PH3) antibody, 1:200 (Millipore, #06-570). Experiments were performed on serial cryosections of 20 μm, 200 μm apart using a minimum of 5 embryos per

genotype. Sections were briefly microwaved to boiling point in 10 mM sodium citrate (pH 6.0) 3 times, for antigen enhancement, cooled, rinsed in 1x PBS, permeablized with 0.1% Triton x-100 blocked in 10% goat serum (GS)/PBS/0.1% Triton x-100 for at least 1h at RT. Sections were then incubated with primary antibodies overnight at 4°C in the same blocking solution reducing the GS to 5%, rinsed, and incubated in secondary antibodies for at least 1h 30 min at RT. The following secondary antibodies were used: For anti-PH3, Alexa Fluor 594-conjugated anti-rabbit, 1:400 (Life Technologies, Invitrogen). For anti-KI67 immunohistochemistry (IHC), sections were also treated with 0.5% H_2O_2 in ethanol to block endogenous peroxidase activity. Anti-KI67, was revealed by incubation with a biotinylated mouse secondary antibody (1:200) and VECTASTAIN Elite-ABC kit reaction (Vector Laboratories) with the TSA-Plus Fluorescein System NEL741001KT (Perkin-Elmer Inc.), following the manufacturer's instructions. Fluorescence was observed with an epifluorescence microscope (Leica DMI6000B, acquisition software LAS AF 2.6). Images were digitally documented with a camera and computer processed using Adobe Photoshop® version 6 for Windows.

Immunohistochemistry (IHC) experiments were performed on serial cryosections of 20 μm, 200 μm apart, using a minimum of 5 embryos per genotype. Sections were briefly post-fixed with 4% PFA in PBS, then rinsed with PBS, permeablized with 0.5% Tween 20, blocked in 20% GS/PBS/0.5% Tween 20 for at least 1h at RT. Sections were then incubated with the primary antibody (rabbit polyclonal anti-TBR1 antibody, 1:200, Millipore, #AB10554) overnight at 4°C in the same blocking solution reducing the GS to 5%, rinsed, and treated with 0.5% H_2O_2 in ethanol to block endogenous peroxidase activity. TBR1-expressing cells were revealed by incubation with biotinylated rabbit secondary antibody (1:200), VECTASTAIN Elite-ABC kit reaction and SK-4100 DAB Substrate Kit (Vector Laboratories), following the manufacturer's instructions. Staining was observed in bright field with a Leica DM6000B microscope (acquisition software LAS V4.1). Images were digitally documented with a camera and computer processed using Adobe Photoshop® version 6 for Windows.

(c) Data quantification.

Cell counts on E13.5 brain sections (IF and IHC): For PH3 quantification, cell counts were performed using the ImageJ cell counter tool on a single hemisphere per embryo (n = 5–6/genotype), comprising nine anatomically matched sections 200 μm apart along the rostral to caudal brain axis. Landmarks: the first five sections were 200 μm apart, starting from the first section in which the lateral ganglionic eminence (LGE) was clearly visible, and before the appearance of the hippocampal primordium. In the mouse strain used here, this position is ∼600 μm caudal to the prospective olfactory bulb (OB). The 6th and 7th sections were 400 μm apart, so as to identify better the CGE domain. Counting box positioning: in the cortex (Cx), three counting boxes of 100 μm^2 spanning the thickness of the Cx, starting from the ventricular surface were positioned in the medio-lateral (ML) cortex, along a line tangential to the LGE or caudal (C) GE (cartoon in **Figure 1**). For KI67 quantification, the ratio between the thickness of the KI67-positive zone and the whole cortical thickness, in the ML cortex, was evaluated on a single hemisphere per embryo (n = 5–6/genotype). Seven sections per hemisphere were evaluated in rostral—caudal sections following the aforementioned landmarks. For TBR1 quantification, sections were processed following the landmarks indicated for *ISH* analysis, and TBR1-positive cells were counted using multiple counting boxes of 100 μm^2 spanning the thickness of the Cx, positioned starting from the ventricular surface in the ML cortex, along a line tangential to the GEs (lateral, medial or caudal at the corresponding levels). Cell counts on adult brain sections immunostained for TBR1: Cryosectioning of adult brains and immunostaining for TBR1 were performed as described for embryonic brain sections. Cell counts were performed on coronal sections of a single hemisphere per animal (8 weeks of age, n = 5/genotype/treatment) using counting boxes 500 μm wide that were placed in the primary somatosensory cortex (S1) around Bregma level 0.50 mm (Paxinos and Franklin, 2012). Boxes spanned the entire thickness of the cortex (white matter to pia) and were divided into 12 equidistant bins. Cell counts are expressed as the average density of TBR1+ cells/100 μm^2 for each bin.

In situ evaluation: For *Tis21*, optical density (OD), minus the slice background OD, was measured on 2D images using the ImageJ graphic pen tool (unit area 50 μm^2). For Pax6 and ND2, we measured the ratio between the thickness of the probe signal and the total thickness of the ML cortex on 2D images using the ImageJ graphic pen tool. Measurements were made at a single position, shown in **Figure 1**, in rostral, medial and caudal sections that were 600 μm apart. Landmarks in coronal sections, rostral—caudal: Rostral: regarding the serial sections collected on each slide, the rostral section selected was the second in which the LGE was clearly visible, before the appearance of the hippocampal primordium (∼800 μm after the appearance of the prospective OB). Medial: ∼600 μm caudal to the rostral slice. The section selected was the first in which the MGE was completely visible, together with the hippocampal primordium detached from the subpallium, the choroid plexus within the left and lateral ventricle and arising from the medial wall. Caudal: ∼600 μm caudal to the medial slice. The section was selected where the CGE was the only GE present. Landmarks for this level are the presence of the thalamus, superior and inferior part of 3rd ventricle, interthalamic adhesion.

Statistical Analysis

The data were statistically analyzed and graphically represented using the Microsoft Office Excel and Prism software. Results are expressed as the mean ± standard deviation (SD). In embryos the Ordinary One Way ANOVA and unpaired Student's t-test with Welch's correction and were used for statistical analysis. For adult brains, the χ^2 test and the unpaired, 2-tailed Student's t-test were used for the statistical analysis. The Benjamini-Hochberg procedure was applied to correct for multiple testing. For all experiments, values of $P \leq 0.05$ were considered to be statistically significant.

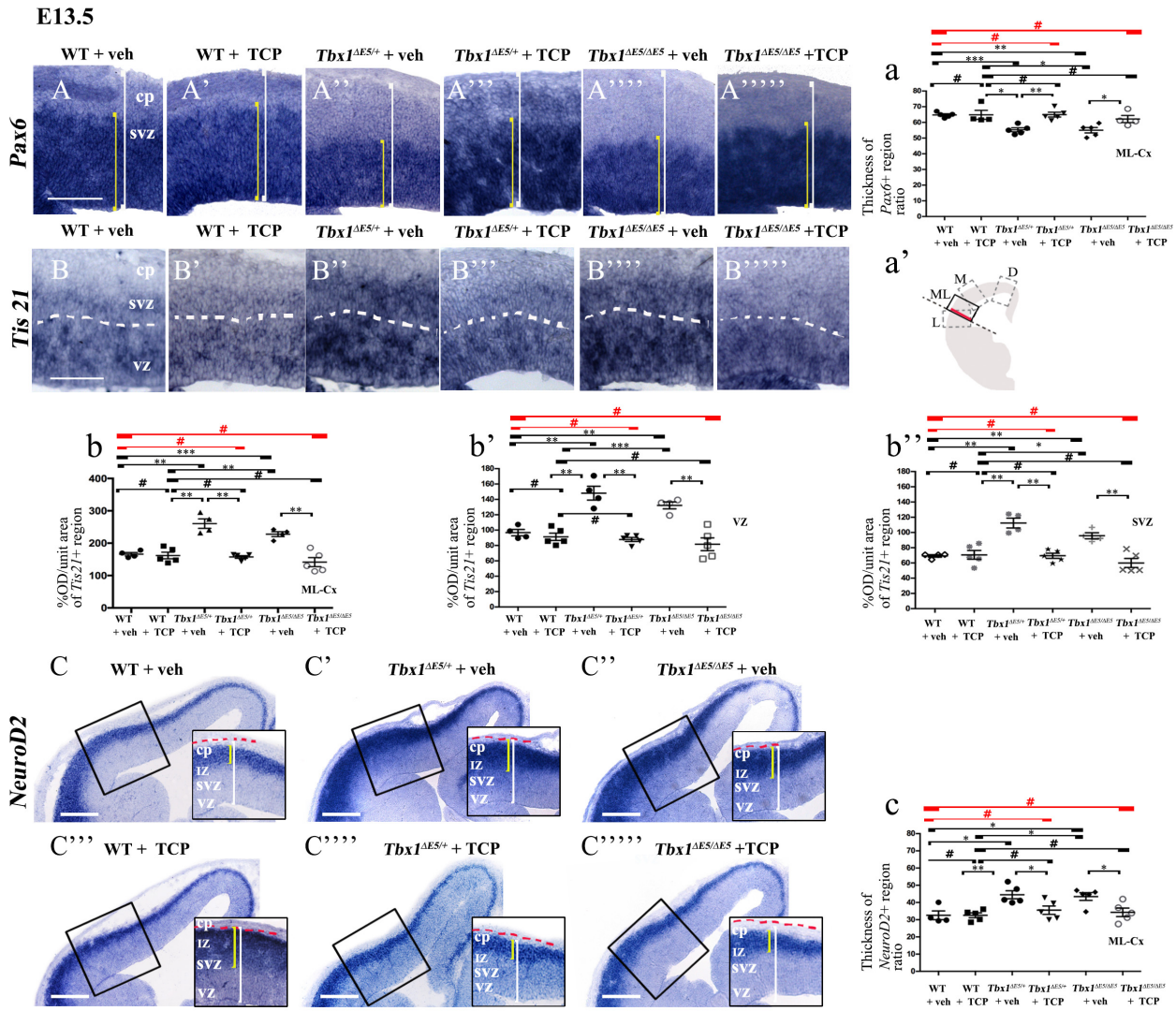

FIGURE 1 | TCP treatment restores normal expression of cortical markers in *Tbx1* mutant embryos. Panels show coronal sections of embryonic brains at E13.5. The cartoon a' indicates the position of the ML-cortex in coronal brain sections (boxed area). The red line indicates the position where all measurements were made. **(A,a)** *In situ* hybridization of *Pax6* **(A–A"")** revealed thinning of the expression domain (yellow brackets) in vehicle-treated $Tbx1^{\Delta E5/+}$ (heterozygous) embryos **(A")** and $Tbx1^{\Delta E5/\Delta E5}$ (homozygous) embryos **(A"")** compared to vehicle-treated WT embryos **(A,a)**, which was rescued by TCP treatment **(A"',A"",a)**. **(B,b)** *In situ* hybridization of *Tis21* **(B–B"")** showed increased expression (OD) in the ML-cortex of vehicle-treated $Tbx1^{\Delta E5/+}$ embryos **(B",b)** and $Tbx1^{\Delta E5/\Delta E5}$embryos **(B"",b)**, compared to vehicle-treated WT embryos **(B,b)**, including the VZ **(b')** and SVZ **(b")**, which was rescued by TCP treatment **(B"',B"", b,b',b")**. **(C,c)** *In situ* hybridization of *NeuroD2* **(C–C"")** showed increased expression in the ML-cortex of vehicle-treated $Tbx1^{\Delta E5/+}$ embryos **(C',c)** and $Tbx1^{\Delta E5/\Delta E5}$embryos **(C",c)** compared to vehicle-treated WT embryos **(C,c)**, and extension of the expression domain (yellow brackets in **C',C"**) relative to the total ventricular pial thickness (white brackets), which was rescued by TCP treatment **(C"",C"",c)**. Scale bars, 100 μm in all panels except panel C, which is 200 μm. $^{*}P \leq 0.05$, $^{**}P \leq 0.01$, $^{***}P \leq 0.001$, error bars indicate mean ± SD, red horizontal bars with # not significant, n = 5–6 per genotype. VZ, ventricular zone; SVZ, subventricular zone; IZ, intermediate zone; CP, cortical plate; ML-Cx, medio-lateral cortex; D, dorsal; M, medial; ML, medio-lateral; L, lateral; OD, optical density.

RESULTS

LSD1/2 Inhibition

Tranylcypromine (TCP) is an LSD1/2 (KDM1A/B) demethylase inhibitor that blocks irreversibly the enzymatic activity of LSD1 (Binda et al., 2002; Shi et al., 2004; Forneris et al., 2005). TCP has been shown to rescue partially the loss of H3K4me1 in $Tbx1^{lacZ/+}$ embryos and partially rescue the cardiovascular phenotype in $Tbx1^{lacZ/+}$ and $Tbx1^{neo2/-}$ embryos (Fulcoli et al., 2016). To test whether TCP rescues or modifies the brain cortex phenotype in *Tbx1* mutants, we intercrossed $Tbx1^{\Delta E5/+}$ animals (heterozygous for *Tbx1*) and pregnant females were injected intraperitoneally (i.p.) with TCP (10 mg Kg^{-1} body weight) or with vehicle (saline solution) at embryonic days (E)10.5, E11.5, and E12.5. We harvested embryos at E13.5 and prepared coronal brain cryosections

TABLE 1 | *P* values for the data shown in the graphs (dot-plots) in **Figure 1**.

Unpaired *t*-test with Welch's correction	WT-veh vs. WT -TCP	WT-veh vs. *Tbx1*$^{\Delta E5/+}$ -veh	WT-TCP vs. *Tbx1*$^{\Delta E5/+}$ -TCP	WT-veh vs. *Tbx1*$^{\Delta E5/+}$ -TCP	WT-veh vs. *Tbx1*$^{\Delta E5/\Delta E5}$ -veh	WT-TCP vs. *Tbx1*$^{\Delta E5/\Delta E5}$ -TCP	WT-veh vs. *Tbx1*$^{\Delta E5/\Delta E5}$ -TCP	Ordinary One Way ANOVA
Pax6	0.9886	0.0005	0.9653	0.913	0.0026	0.497	0.3394	0.0002
Tis21	0.4105 (vz), 0.8255 (svz) 0.7327 (tot)	0.0057 (vz), 0.005 (svz) 0.0048 (tot)	0.5466 (vz), 0.8697 (svz) 0.6949 (tot)	0.1218 (vz) 0.9477 (svz) 0.2333 (tot)	0.0011 (vz), 0.0037 (svz) 0.0009 (tot)	0.3476 (vz), 0.2341 (svz) 0.2471 (tot)	0.1546 (vz), 0.196 (svz) 0.1604 (tot)	< 0.0001 (vz + svz) < 0.0001 (tot)
NeuroD2	0.9948	0.0116	0.3317	0.4322	0.0163	0.5597	0.6419	0.0035

for marker analyses. Our previous study has shown that *Tbx1* mutants (heterozygous and homozygous loss of function) have brain cortex abnormalities that we have hypothesized to result from premature differentiation of cortical neurons (Flore et al., 2017). In the current study, we evaluated phenotypic rescue of the cortical abnormalities based on the expression of a subset of the molecular markers used by Flore et al., 2017, including, *Pax6*, *Tis21*, and *NeuroD2*. *Pax6* labels apical neural progenitors (AP) in the ventricular zone (VZ) of the cortex; its expression domain was thinned in *Tbx1* mutant embryos. *Tis21* identifies neurogenic progenitors, i.e., APs switching from symmetric self-renewing divisions to neurogenic divisions, and basal progenitors (BP) undergoing neurogenic divisions. Expression of *Tis21* was increased in

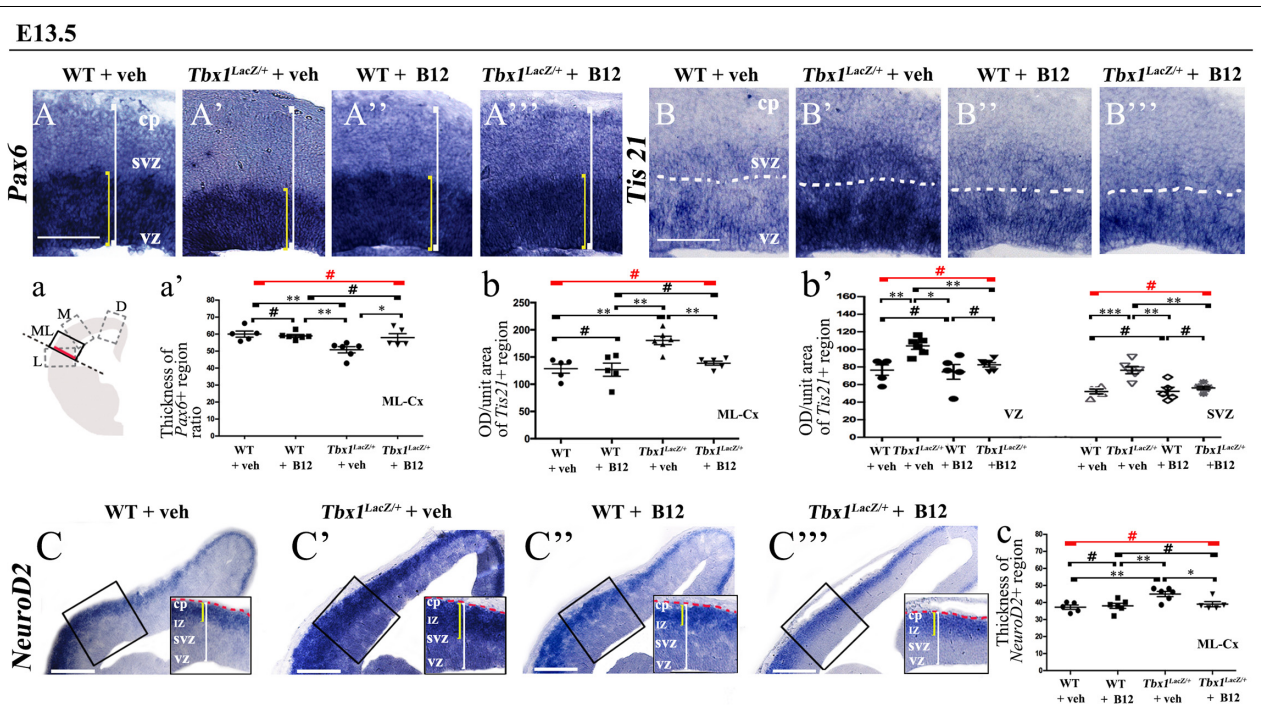

FIGURE 2 | Vitamin B12 treatment restores normal expression of cortical markers in *Tbx1* heterozygous embryos. Panels show coronal sections of embryonic brains at E13.5. The cartoon, a, indicates the position of the ML-cortex in coronal brain sections (boxed area). The red line indicates the position where all measurements were made. **(A,a)** *In situ* hybridization of *Pax6* **(A–A''')** revealed thinning of the expression domain (yellow brackets) in vehicle-treated *Tbx1*$^{lacZ/+}$ (heterozygous) embryos **(A')** compared to vehicle-treated WT embryos **(A,a)**, which was rescued by B12 treatment **(A''',a)**. **(B,b,b')** *In situ* hybridization of *Tis21* **(B–B''')** showed increased expression (OD) in the ML-cortex of vehicle-treated *Tbx1*$^{lacZ/+}$ embryos compared to vehicle-treated WT embryos **(B)**, including the VZ and SVZ **(B',b,b')**, which was rescued by B12 treatment **(B''',b,b')**. **(C,c)** *In situ* hybridization of *NeuroD2* **(C–C''')** showed increased expression in the ML-cortex of vehicle-treated *Tbx1*$^{lacZ/+}$ embryos **(C',c)** compared to vehicle-treated WT embryos **(C)** and extension of the expression domain (yellow brackets), relative to the total ventricular pial thickness (white brackets), which was rescued by B12 treatment **(C''',c)**. Dashed red line defines the external edge of the cortical plate (CP). Scale bars, 100 μm in all panels except **(C)**, which is 200 μm. $^{*}P \leq 0.05$, $^{**}P \leq 0.01$, $^{***}P \leq 0.001$, error bars indicate mean ± SD, red horizontal bars with # not significant, $n = 5$–6 per genotype. VZ, ventricular zone; SVZ, subventricular zone; IZ, intermediate zone; CP, cortical plate; ML-Cx, medio-lateral cortex; D, dorsal; M, medial; ML, medio-lateral; L, lateral; OD, optical density.

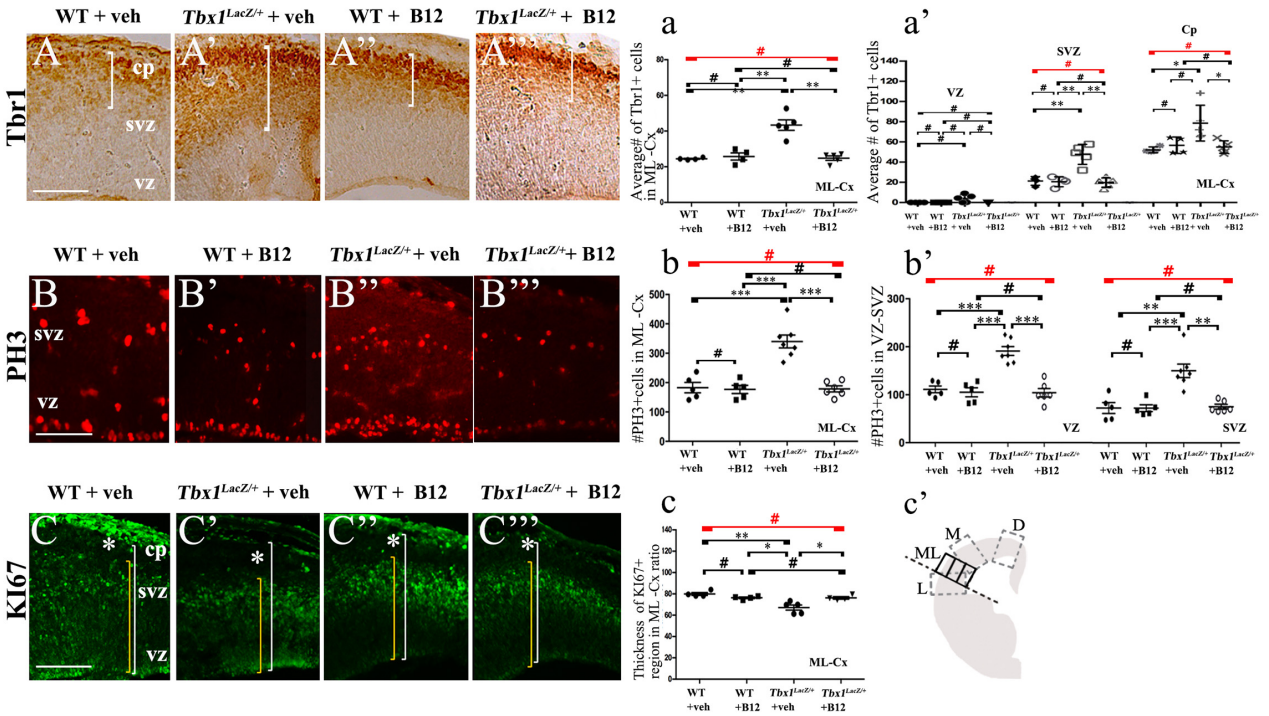

FIGURE 3 | Vitamin B12 treatment restores normal expression of cortical markers in *Tbx1* heterozygous embryos. Panels show coronal sections of embryonic brains at E13.5. **(A,a)** Immunostaining for TBR1 **(A–A")** revealed the precocious presence of terminally differentiated neurons in the SVZ of $Tbx1^{lacZ/+}$ embryos **(A')**. White brackets define the regions containing TBR1-positive cells in **(A,A')**. Quantitative analysis confirmed the altered distribution and frequency of mature cortical neurons in the ML-cortex, of $Tbx1^{lacZ/+}$ embryos, including the SVZ and CP **(a)**, which was rescued by B12 treatment **(A"',a)**. **(B,b)** Immunostaining for phospho-histone 3 (PH3) revealed increased mitotic activity in the proliferative zones (VZ, SVZ) of the ML-cortex of vehicle-treated $Tbx1^{lacZ/+}$ embryos **(B',b,b')** compared to vehicle-treated WT embryos **(B,b)**, which was rescued by B12 treatment **(B"',b,b')**. **(C,c)** Immunostaining for KI67. White asterisks identify KI67-negative regions. Quantitative analysis **(c)** revealed the reduced thickness of the KI67- expressing region (yellow brackets) relative to the total ventricular-to-pial thickness (white brackets) in vehicle-treated $Tbx1^{lacZ/+}$ embryos **(C',c)** compared to vehicle-treated WT embryos **(C)**, which was rescued by B12 treatment **(C"',c)**. The cartoon **(c')** indicates the position of the ML-cortex in coronal sections, and the position of the counting boxes for cell counts. Scale bars, 100 μm. $^{*}P \leq 0.05$, $^{**}P \leq 0.01$, $^{***}P \leq 0.001$, error bars indicate mean ± SD, red horizontal bars with # not significant, n = 5–6 per genotype. VZ, ventricular zone; SVZ, subventricular zone; CP, cortical plate; ML-Cx, medio-lateral cortex; D, dorsal; M, medial; ML, medio-lateral; L, lateral.

Tbx1 mutant embryos. *NeuroD2* labels fully differentiated neurons; its expression domain is expanded in *Tbx1* mutant embryos (Flore et al., 2017). Analysis of these markers in *Tbx1* mutant embryos confirmed these previously reported expression anomalies and showed that TCP treatment fully rescued their expression in $Tbx1^{+/\Delta E5}$ and $Tbx1^{\Delta E5/\Delta E5}$ embryos, i.e., their expression returned to WT levels (**Figures 1A**, 1a, *Pax6*; **Figures 1B**, 1b, *Tis21*; **Figures 1C**, 1c, *NeuroD2*, and **Table 1**). Moreover, WT embryos treated with vehicle or with TCP showed no differences in the cortical expression of *Pax6, Tis21* and *NeuroD2*, indicating that TCP alone does not influence cortical development (**Figure 1a**, *Pax6*; **Figure 1b**, *Tis21*; **Figure 1c**, *NeuroD2*, and **Table 1**). Finally, $Tbx1^{\Delta E5/+}$ and $Tbx1^{\Delta E5/\Delta E5}$ embryos treated with vehicle showed similar alterations in expression of *Pax6, Tis21* and *NeuroD2* as those previously reported by Flore et al. (2017) (**Figure 1a**, *Pax6*; **Figure 1b**, *Tis21*; **Figure 1c**, *NeuroD2*, and **Table 1**).

Vitamin B12 Treatment

Vitamin B12 (B12) was identified in a high throughput screen to identify small molecules that enhanced *Tbx1* gene expression in *Tbx1* heterozygous mouse embryonic fibroblasts (Lania et al., 2016). The authors of this study reported the partial rescue of cardiovascular phenotypes in mid- and pre-term *Tbx1* mutant embryos when treated with high doses of B12. B12 is an essential vitamin that plays an important role in cellular metabolism through its effects on DNA synthesis, methylation and mitochondrial metabolism. Cases of clinically severe B12 deficiency, such as pernicious anemia, have revealed the critical role of this vitamin for hemopoiesis and for brain development and function (Green et al., 2017).

To test whether B12 treatment rescues or modifies the brain cortex phenotype in *Tbx1* mutants, we crossed male $Tbx1^{lacZ/+}$ mice with female WT mice and pregnant females were injected i.p. with B12 (20 mg/Kg^{-1} body weight) or with the same volume of vehicle (PBS) daily from E7.5 to

TABLE 2 | *P* values for the data shown in the graphs (dot-plots) in **Figure 2** and **Figure 3**.

Unpaired *t*-test with Welch's correction	WT-veh vs. WT B12	WT-veh vs. *Tbx1*$^{LacZ/+}$-veh	WT-B12 vs. *Tbx1*$^{Lacz/+}$-B12	WT-veh vs. *Tbx1*$^{LacZ/+}$-B12	Ordinary One Way ANOVA
Pax6	0.6073	0.0059	0.7118	0.5061	0.0047
Tis21	0.8485 (vz), 0.9754 (svz) 0.903 (tot)	0.0056 (vz), 0.0009 (svz) 0.0015 (tot)	0.404 (vz), 0.4688 (svz) 0.3908 (tot)	0.3889 (vz), 0.2299 (svz) 0.3134 (tot)	0.0029 (vz) 0.0002 (svz) 0.0004 (tot)
NeuroD2	0.705	0.0037	0.6428	0.3978	0.0047
PH3	0.628 (vz), 0.9884 (svz) 0.793 (tot)	< 0.0001 (vz), 0.0015 (svz) 0.0002 (tot)	0.9342 (vz), 0.7426 (svz) 0.9194 (tot)	0.511 (vz), 0.8316 (svz) 0.08401 (tot)	(<0.0001 (vz), (<0.0001 (svz) (<0.0001 (tot)
KI67	0.0764	0.0033	0.9379	0.0867	0.0007
Tbr1	0.8256 (svz) 0.3504 (cp) 0.568 (tot)	0.0021 (svz) 0.0278 (cp) 0.0029 (tot)	0.7952 (svz) 0.7296 (cp) 0.7193 (tot)	0.5992 (svz) 0.4016 (cp) 0.7648 (tot)	<0.0001 (svz) 0.0073 (cp) <0.0001 (tot)

E11.5. We harvested embryos at E13.5 and prepared serial coronal brain cryosections. We first measured the thickness of the ML-cortex in B12-treated vs. vehicle-treated (control) embryos, and found no difference between any of genotypes or treatment groups (**Supplementary Figure 1**). The remaining serial sections were subjected to ISH with probes against *Pax6, Tis21,* and *NeuroD2*, and immunostaining with anti-TBR1 antibody, which labels terminally differentiated cortical neurons. The results obtained with these markers, which are shown in **Figures 2**, **3**, and summarized in **Table 2**, were similar overall to those obtained with TCP treatment. Specifically, in *Tbx1*$^{lacZ/+}$ embryos, B12 treatment fully rescued the cortical expression of *Pax6, Tis21* and *NeuroD2*, compared to those treated with vehicle (**Figures 2A**', 2A", 2a', *Pax6*; **Figures 2B**', 2B"', 2b, 2b', *Tis21*; **Figures 2C**', 2C"', 2c, *NeuroD2,* and **Table 2**). Moreover, WT embryos treated with the vehicle or with B12 showed no differences in cortical expression of these markers, indicating that B12 alone does not affect cortical development (**Figures 2A**, 2A", 2a', *Pax6*; **Figures 2B**, 2B", 2b, 2b', *Tis21*; **Figures 2C**, 2C", 2c, *NeuroD2,* and **Table 2**). Finally, *Tbx1*$^{lacz/+}$ embryos treated with vehicle showed similar alterations in expression of *Pax6, Tis21*, *NeuroD2* as those previously reported by Flore et al., 2017 (**Figures 2A**', 2a, *Pax6*; **Figures 2B**', 2b, 2b', *Tis21*; **Figures 2C**', 2c, *NeuroD2,* and **Table 2**). Expression of TBR1 was also normalized in B12 treated *Tbx1*$^{lacZ/+}$ embryos compared to those treated with vehicle (**Figures 3A**', 3A"', 3a, 3a').

In order to obtain a broader picture of the efficacy of B12 treatment, we looked for rescue of the cell proliferation/cell cycle anomalies, which are part of the cortical phenotype observed in *Tbx1* mutants (Flore et al., 2017). For this, we immunostained brain cryosections for phospho-histone 3 (PH3), which labels mitotic cells (M phase) and KI67, which labels cycling cells, i.e., not in G0. Flore et al., 2017 reported an increased number of PH3+ cells in the proliferating layers of the cortex in *Tbx1* mutants at E13.5, and an expanded KI67-negative layer where terminally differentiated neurons reside. We found that B12 treatment fully rescued both of these cellular phenotypes in the cortex of *Tbx1*$^{lacz/+}$ embryos (**Figures 3B**', 3B"', 3b, 3b', PH3; **Figures 3C**', 3C"', 3c, KI67, and **Table 2**). Together, these results indicate that B12 treatment has high efficacy in the developing murine cortex.

We next tested whether B12 treatment during embryogenesis rescues cortical abnormalities in adult *Tbx1* mutant mice. For this, we crossed male *Tbx1*$^{lacZ/+}$ mice with female WT mice and treated pregnant females with B12 as described above from E7.5 to E11.5. The brains of B12-treated and untreated (NT) *Tbx1*$^{lacZ/+}$ and WT mice were collected at 8 weeks of age and serial coronal brain sections were immunostained with anti-TBR1 antibody. We selected TBR1 as the marker of choice for these experiments because our previous study revealed a striking difference in the distribution of TBR1+ projection neurons in the S1 cortex (cartoon in **Figure 4**) of *Tbx1*$^{lacZ/+}$ adult mice compared to WT littermates (Flore et al., 2017). Results showed that B12 treatment rescued the abnormal distribution of TBR1+ cells in the S1 cortex of *Tbx1*$^{lacZ/+}$ mutants (**Figures 4A–F**). Indeed, there was no difference in the distribution of TBR1+ cells in the S1 cortex (12 counting bins) between B12-treated *Tbx1*$^{lacZ/+}$ mice and untreated WT mice (**Figure 4I**) and the sparse distribution of TBR1+ cells in cortical layer V was restored in B12-treated *Tbx1*$^{lacZ/+}$ animals (**Figure 4D**). These data indicate that the beneficial effect of B12 treatment during embryogenesis is maintained into adulthood, at least as measured by the TBR1 marker.

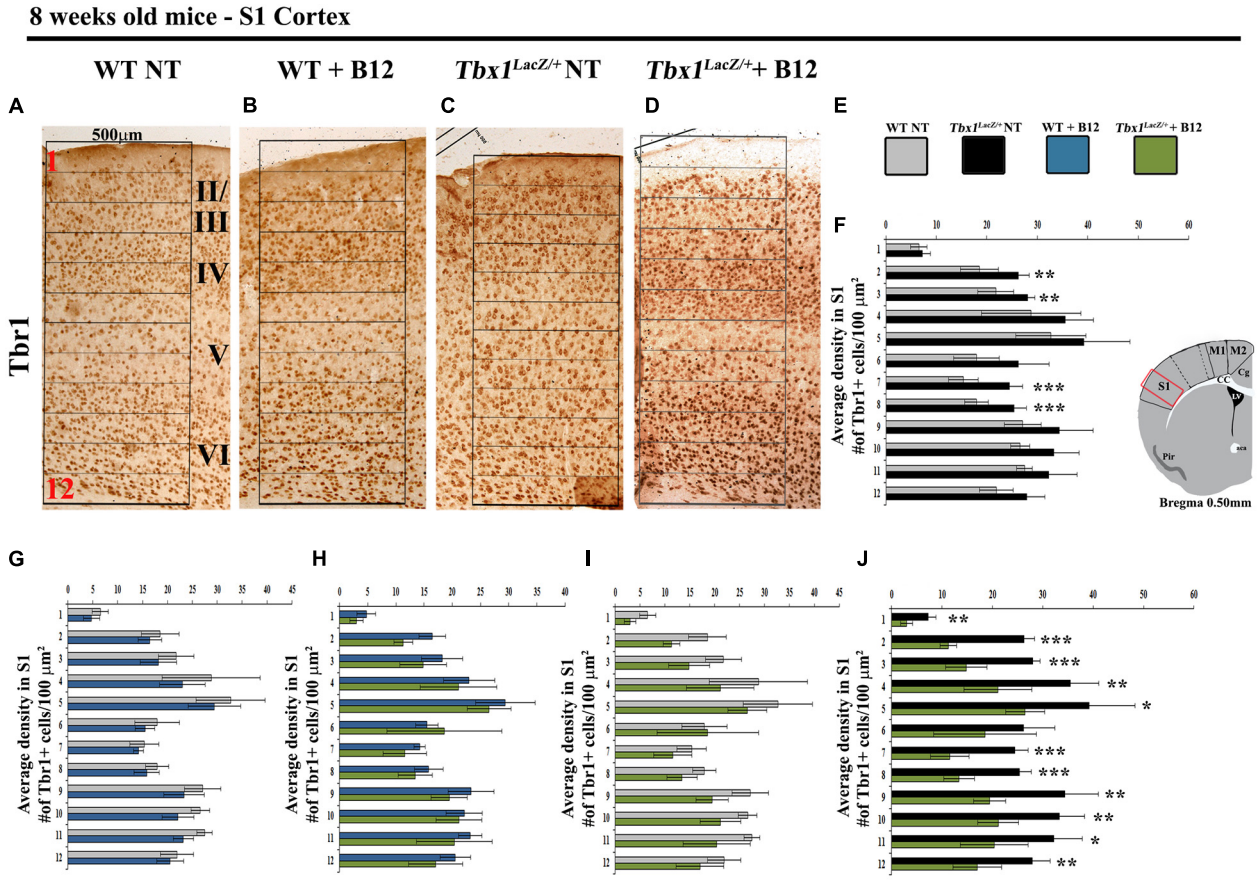

FIGURE 4 | Vitamin B12 treatment restores normal distribution of TBR1-expressing cells in the adult S1 cortex in *Tbx1* heterozygous mice. **(A–D)** Coronal brain sections of the somatosensory (S1) cortex of young adult mice (8 weeks of age) immunostained for TBR1. Enhanced frequency of TBR1+ cells in the granular and infragranular layers (bins 2, 3, 7 and 8) in the $Tbx1^{lacZ/+}$ brain **(C)** compared to untreated (NT) wild type **(A)** mice (**F**, $\chi^2 = 26.55$, df = 11, $P \leq 0.01$), is rescued by B12 treatment **(D)** (**I**, $\chi^2 = 18.375$, df = 11, 0.10, $P < 0.25$). Roman numerals indicate the cortical layers I–VI, Arabic numerals indicate the position of the 12 bins used for quantification. **(E)** Color scheme for the genotypes shown in the histograms **(F–J)**. **(F–J)** Pairwise comparisons of the average distribution of TBR1-expressing cells in the 12 bins spanning the S1 cortex of mice with the genotypes indicated in **(E)**, $n = 5$ per genotype. The cartoon in F indicates the position of the S1 cortex (boxed area) in coronal brain sections of adult mice, at Bregma level 0.50 mm, where all measurements were made. $^*P \leq 0.05$, $^{**}P \leq 0.01$, $^{***}P \leq 0.001$, error bars indicate mean ± SD. *P*-values in **(F,I)** have been corrected by the Benjamini Hochberg procedure.

In order to understand whether B12 treatment restores normal gene expression and normal cortical cytoarchitecture through a mechanism that does not depend upon the transcriptional increase of *Tbx1*, we intercrossed $Tbx1^{lacZ/+}$ mice and treated pregnant females with B12 using the same experimental conditions as those described for *Tbx1* heterozygous embryos. Surprisingly, we found that in B12-treated $Tbx1^{lacZ/lacZ}$ embryos, the cortical expression of *Pax6, Tis21*, *NeuroD2,* and PH3 was fully rescued, compared to $Tbx1^{lacZ/lacZ}$ embryos treated with the vehicle (**Figures 5A**', 5A", 5a, *Pax6*; **Figures 5B**', 5B", 5b, 5b', *Tis21*; **Figures 5C**', 5C", 5c, *NeuroD2*; **Figures 5D**', 5D", 5d, 5d', PH3, and **Table 3**). These results demonstrate that the phenotypic rescue obtained with B12 does not depend solely upon the transcriptional increase of *Tbx1*. **Figure 5E** shows a model of the possible interactions between TBX1 and B12 that could account for the phenotypic rescue.

DISCUSSION

Our study shows for the first time that anomalies of cortical cytoarchitecture caused by *Tbx1* mutation can be prevented by appropriate pharmacological intervention during gestation. We tested two compounds that have been shown to reduce the frequency and severity of cardiovascular defects in *Tbx1* mutant mice, namely TCP and B12. We found that treatment with either compound fully restored the normal expression of a set of cortical markers that is anomalously expressed in *Tbx1* mutant embryos. We focused our attention on the rescue of the phenotypes affecting cortical progenitors (APs and BPs) and their progeny that were described by Flore et al. (2017). The study by Flore et al. showed that the cortical phenotype was fully penetrant and had a similar severity in $Tbx1^{lacZ/+}$ and $Tbx1^{lacZ/lacZ}$ embryos at E13.5. In the current study, we found that this was also the case for a second *Tbx1* allele, $Tbx1^{\Delta E5}$ which is a null allele resulting

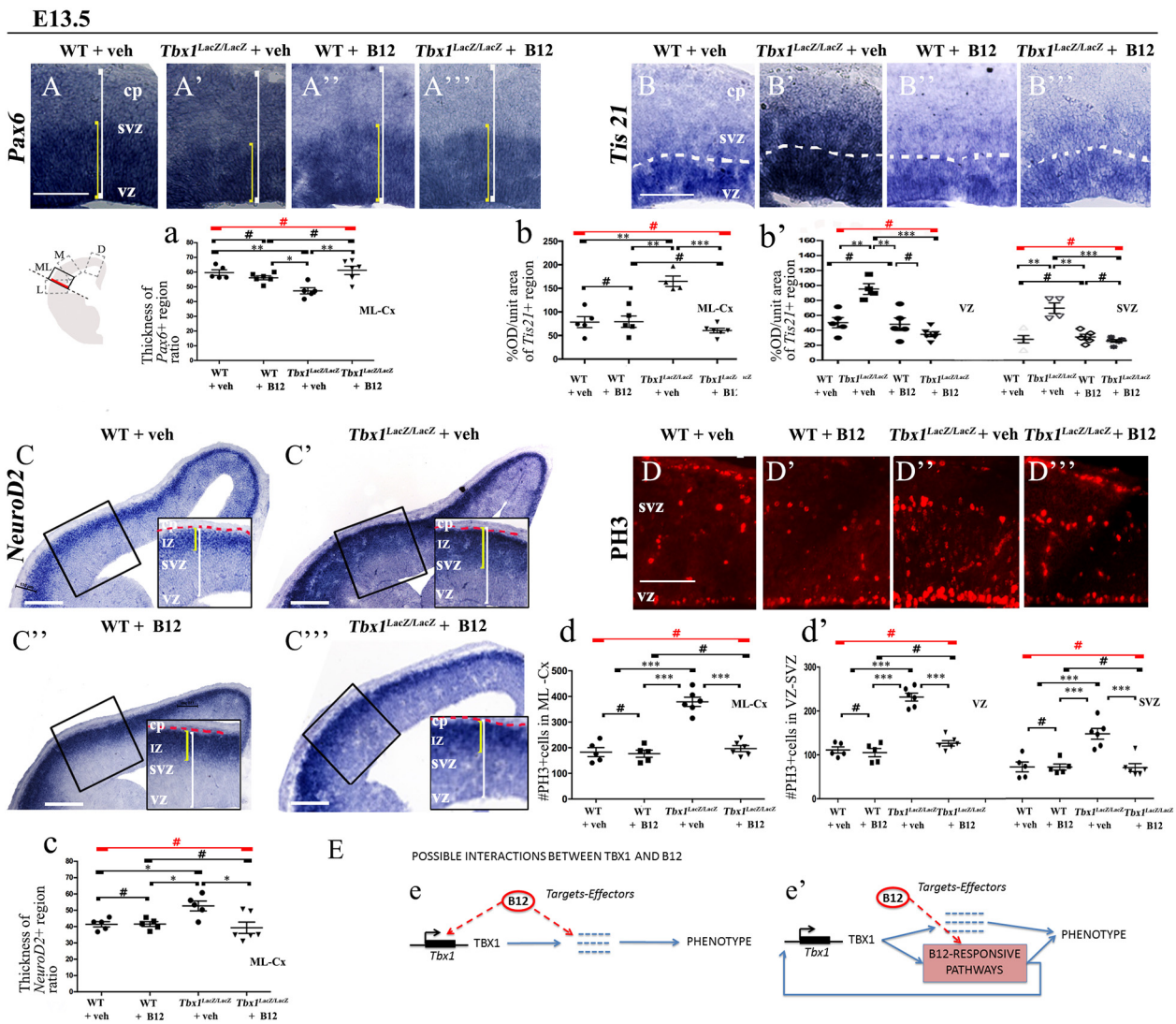

FIGURE 5 | Vitamin B12 treatment restores normal expression of cortical markers in *Tbx1* homozygous embryos. All panels show coronal sections of embryonic brains at E13.5. The cartoon in **(A)** indicates the position of the ML-cortex in coronal brain sections (boxed area). The red line indicates the position where all measurements were made. **(A,a)** *In situ* hybridization of *Pax6* **(A–A"')** revealed thinning of the expression domain (yellow brackets) in vehicle-treated *Tbx1*$^{lacZ/lacZ}$ embryos **(A')** compared to WT **(A,a)**, which was rescued by B12 treatment **(A"',a)**. **(B,b,b')** *In situ* hybridization of *Tis21* **(B–B"')** showed increased expression in the ML-cortex of *Tbx1*$^{lacZ/lacZ}$ embryos, including the VZ and SVZ **(B',b,b')**, which was rescued by B12 treatment **(B"',b,b')**. Dashed white line indicates border between the VZ and SVZ. **(C,c)** *In situ* hybridization of *NeuroD2* **(C–C"')** showed increased expression in the ML-cortex of *Tbx1*$^{lacZ/lacZ}$ embryos **(C',c)** and extension of the expression domain (yellow brackets) relative to the total ventricular pial thickness (white brackets), which was rescued by B12 treatment **(C"',c)**. Dashed red line defines the external edge of the CP. **(D,d,d')** Immunostaining for phosphohistone 3 (PH3) revealed increased mitotic activity in the proliferative zones (VZ, SVZ) of the ML-cortex of *Tbx1*$^{lacZ/lacZ}$ embryos **(D',d,d')**, which was rescued by B12 treatment **(D"',d,d')**. **(E)** Alternative models of interactions between TBX1 and B12 that are consistent with the observed phenotypic rescue in *Tbx1* homozygous mutants. In **(e)**, B12 acts by altering the expression of genes, including *Tbx1,* and one or more critical TBX1 targets. The latter activity is retained when *Tbx1* expression is abolished. In **(e')**, B12 acts downstream of TBX1, on one or more critical pathways that respond to TBX1 and has a positive feedback on *Tbx1* expression. In the absence of TBX1, B12 continues to affect (activate or repress) the critical pathways. Scale bars, 100 μm in all panels except panel C, which is 200 μm. $^{*}P \leq 0.05$, $^{**}P \leq 0.01$, $^{***}P \leq 0.001$, error bars indicate ± SD, red horizontal bars with # not significant, n = 5–6 per genotype. VZ, ventricular zone; SVZ, subventricular zone; IZ, intermediate zone; CP, cortical plate; ML-Cx, medio-lateral cortex; D, dorsal; M, medial; ML, medio-lateral; L, lateral; OD, optical density.

from the recombination of the *Tbx1*^{flox} allele (Xu et al., 2004). Furthermore, for both alleles, and for both drugs, the phenotypic rescue was complete, for the markers tested. This is in contrast to the cardiovascular phenotype, for which only partial rescue was obtained (Fulcoli et al., 2016; Lania et al., 2016). Thus, the brain seems to be more sensitive than the heart to the beneficial effects of these two drugs. In the study by Fulcoli et al. (2016) only about one third of the genes, the expression of which was disrupted in

TABLE 3 | *P* values for the data shown in the graphs (dot-plots) in **Figure 5**.

Unpaired *t*-test with Welch's correction	WT-veh vs. WT B12	WT-veh vs. $Tbx1^{LacZ/lacZ}$ - veh	WT-B12 vs. $Tbx1^{LacZ/LacZ}$ - B12	WT-veh vs. $Tbx1^{LacZ/LacZ}$ - B12	Ordinary One Way ANOVA
Pax6	0.1739	0.0027	0.1513	0.6634	0.0014
Tis21	0.851 (vz), 0.6412 (svz) 0.960 (tot)	0.0.003 (vz), 0.0036 (svz) 0.0011 (tot)	0.1949 (vz), 0.2546 (svz), 0.2054 (tot)	0.0871 (vz), 0.6768 (svz), 0.2086 (tot)	<0.0001 (vz) <0.0001 (svz) <0.0001 (tot)
NeuroD2	0.9544	0.0169	0.5735	0.5996	0.0111
PH3	0.628 (vz), 0.9884 (svz) 0.793 (tot)	<0.0001 (vz), 0.0014 (svz) <0.0001 (tot)	0.0995 (vz), 0.9148 (svz) 0.3048 (tot)	0.1355 (vz), 0.9214 (svz) 0.5365 (tot)	<0.0001 (vz), <0.0001 (svz) <0.0001 (tot)

cells with *Tbx1* knockdown, were rescued by TCP treatment. This might account, at least in part, for the incomplete phenotypic rescue obtained. In the cortex, the greater phenotypic rescue obtained with TCP (and with B12) might be due to a greater recovery of target gene expression, or TBX1 might have different critical targets in brain that are more sensitive to these drugs. Currently, the identity of the Tbx1-dependent cell population that is critical for cortical development in unknown, other than it is mesodermal in origin (Flore et al., 2017).

The rescue of the cortical phenotype in *Tbx1* homozygous mutants treated with TCP was not altogether surprising, since TCP is predicted to function downstream of TBX1 by reducing the H3K4me1 depletion caused by *Tbx1* loss of function (Fulcoli et al., 2016), i.e., through a non-transcriptional mechanism. However, the full phenotypic rescue obtained with B12 treatment was quite unexpected, given that B12 was identified for its ability to enhance *Tbx1* expression. Thus, our study indicates that B12, in addition to acting by transcriptionally increasing *Tbx1* expression, also acts by other as yet unknown mechanisms that favor phenotypic rescue. What might those mechanisms be? One possibility is that in the absence of *Tbx1*, B12 acts on one or more target genes that are also targeted by TBX1, perhaps by altering DNA or histone methylation, or other epigenetic mechanism. Alternatively, B12 might correct a metabolic abnormality caused by the loss of TBX1. Therefore, the possible mechanisms by which B12 acts in rodents are at least three, transcriptional, epigenetic and metabolic, as shown in the model in **Figure 5**. Additional studies will be needed to elucidate which of the potential mechanisms are important for cortical development. Interestingly, a distinct metabolic profile has been reported for children with 22q11.2DS (Napoli et al., 2015), including abnormal levels of multiple metabolites in pathways that are B12-dependent.

How might TCP rescue the cortical phenotype in *Tbx1* mutants? Any proposed mechanism must be compatible with existing knowledge of TBX1 and LSD1 function in this context. For example, in the mouse, *Tbx1* is required in the embryonic medio-lateral (ML) cortex (precursor of the somatosensory cortex) for the differentiation and migration of glutamatergic and GABAergic neurons, a role that is cell non-autonomous and mesoderm-dependent (Flore et al., 2017). From an epigenetic point of view, TBX1 has been shown to recruit histone methyltransferases (HMT) to primed enhancers, rather than to active enhancers, and at some chromatin sites it co-localizes with LSD1, although these sites have not been mapped. Mutation of *Tbx1* in cultured cells and *in vivo* was associated with reduced H3K4me1 at target loci, and this was rescued partially by TCP treatment, as was the cardiovascular phenotype in *Tbx1* mutant embryos (Fulcoli et al., 2016). We propose a model where TBX1, HMTs, and LSD1 co-localize at one or more enhancers of an unknown mesodermally expressed extracellular signal gene (ECS), activating its expression and thereby promoting appropriate differentiation of cortical progenitors in the ML-cortex. In *Tbx1* mutant embryos, the reduced presence of TBX1 and HMTs at the enhancer/s, while maintaining LSD1, reduces levels of H3K4me1 locally causing, or contributing to, a repressive chromatin environment, and silencing of the ECS gene. TCP treatment, by blocking LSD1, counteracts the reduced H3K4 methylation caused by *Tbx1* mutation and restores expression of the ECS gene and thereby appropriate neuronal differentiation. Alternatively, B12 and/or TCP might directly affect a cell differentiation process. We hypothesized that the changes in cortical cytoarchitecture observed in *Tbx1* mutants are the consequence of premature differentiation of cortical progenitors, but this hypothesis will have to be tested directly in the future.

TCP and B12 can now be added to a growing list of drugs and compounds with proven ability to ameliorate the neuronal and/or behavioral deficits found in mouse models of 22q11.2DS (Tamura et al., 2016; Nilsson et al., 2018; Fernandez et al., 2019; Mukherjee et al., 2019; Armando et al., 2020) and, in one case, in patients with 22q11.2DS (Armando et al., 2020). To our knowledge, this study is the first to identify drugs that target *TBX1*, the major candidate gene for 22q11.2DS, that have preventative potential in the mouse model. TCP is not an ideal therapeutic agent because

it lacks specificity for LSD1; it was originally approved by the United States Food and Drug Administration (FDA) for the treatment of depression based on its ability to inhibit monoamine oxidase (MAO). However, numerous TCP derivatives have been developed that have greater specificity for LSD1, some of which are in clinical trials for cancer therapy, reviewed in Fang et al. (2019).

B12 is an exciting therapeutic candidate because it is an approved drug, including for prenatal use, that is inexpensive and virtually harmless, even at high doses. If proven effective in the clinical setting, it would be an important advance over current therapeutic options, which are limited to treating symptoms. In the meantime, mouse studies will continue to provide critical information about the optimal timing of B12 treatment, or indeed of any other therapy, given that we do not know whether the brain-related abnormalities in 22q11.2DS patients, or in the mouse model, are preventable using post-natal treatment, or whether they are the irreversible consequences of abnormal prenatal development. Our data indicate that prenatal treatment normalizes at least some cortical phenotypes observed in adult *Tbx1* mutant mice. It will be of great interest, and of more direct clinical relevance, to establish whether postnatal treatment is also beneficial for behavioral abnormalities, also present in this mouse model (Paylor et al., 2006). Finally, given the proven preventive potential of high dose B12 treatment in the mouse, biochemical analysis of patients would be appropriate to determine whether they have B12 deficiency or in B12-dependent pathways.

DATA AVAILABILITY STATEMENT

The raw data supporting the conclusions of this article will be made available by the authors, without undue reservation.

ETHICS STATEMENT

The animal study was reviewed and approved by the Italian Istituto Superiore di Sanità and Italian Ministero della Salute.

AUTHOR CONTRIBUTIONS

EI and AB designed the study. IF and GF performed the experiments. SC and GL assisted with experiments. EI, IF, and GF analyzed the data. EI wrote the manuscript. All authors contributed to the article and approved the submitted version.

FUNDING

The study was supported by grants from the Jerome Lejeune Foundation, Project No. 1685 to EI, the Leducq Foundation Transatlantic Network of Excellence in Cardiovascular Research, 15CVD01 to EI and AB, and the Ministero dell'Istruzione dell'Università e della Ricerca (MUIR), #20179J2P9J to EI and AB.

ACKNOWLEDGMENTS

We are grateful for the invaluable support of the staff of the IGB-CNR mouse facility and the Integrated Microscopy facility.

SUPPLEMENTARY MATERIAL

The Supplementary Material for this article can be found online at: https://www.frontiersin.org/articles/10.3389/fnmol.2021.663598/full#supplementary-material

Supplementary Figure 1 | Thickness of ML-cortex is not altered in *Tbx1* mutant embryos at E13.5. The cartoon **(A)** indicates the position of the ML-cortex in coronal brain sections (boxed area) at E13.5. The red line indicates the position where cortical thickness (ventricular-to-pial surface) was measured. Cortical thickness was similar in all genotypes and treatment groups that included B12-treated and vehicle-treated $Tbx1^{lacZ/+}$ embryos **(B)** or $Tbx1^{lacZ/lacZ}$ embryos **(C)**.

REFERENCES

Armando, M., Ciampoli, M., Padula, M. C., Amminger, P., De Crescenzo, F., Maeder, J., et al. (2020). Favorable effects of omega-3 polyunsaturated fatty acids in attentional control and conversion rate to psychosis in 22q11.2 deletion syndrome. *Neuropharmacology* 168:107995. doi: 10.1016/j.neuropharm.2020.107995

Binda, C., Mattevi, A., and Edmondson, D. E. (2002). Structure-function relationships in flavoenzyme-dependent amine oxidations: a comparison of polyamine oxidase and monoamine oxidase. *J. Biol. Chem.* 277, 23973–23976. doi: 10.1074/jbc.r200005200

Braunstein, E. M., Monks, D. C., Aggarwal, V. S., Arnold, J. S., and Morrow, B. E. (2009). Tbx1 and Brn4 regulate retinoic acid metabolic genes during cochlear morphogenesis. *BMC Dev. Biol.* 9:31. doi: 10.1186/1471-213X-9-31

Calmont, A., Ivins, S., Van Bueren, K. L., Papangeli, I., Kyriakopoulou, V., Andrews, W. D., et al. (2009). Tbx1 controls cardiac neural crest cell migration during arch artery development by regulating Gbx2 expression in the pharyngeal ectoderm. *Dev. Camb. Engl.* 136, 3173–3183. doi: 10.1242/dev.028902

Caprio, C., and Baldini, A. (2014). p53 suppression partially rescues the mutant phenotype in mouse models of DiGeorge syndrome. *Proc. Natl. Acad. Sci U S A.* 113, 13385–13390. doi: 10.1073/pnas.1401923111

Fagman, H., Liao, J., Westerlund, J., Andersson, L., Morrow, B. E., and Nilsson, M. (2007). The 22q11 deletion syndrome candidate gene Tbx1 determines thyroid size and positioning. *Hum. Mol. Genet.* 16, 276–285. doi: 10.1093/hmg/ddl455

Fang, Y., Liao, G., and Yu, B. (2019). LSD1/KDM1A inhibitors in clinical trials: advances and prospects. *J. Hematol. Oncol.* 12:129.

Fernandez, A., Meechan, D. W., Karpinski, B. A., Paronett, E. M., Bryan, C. A., Rutz, H. L., et al. (2019). Mitochondrial dysfunction leads to cortical under-connectivity and cognitive impairment. *Neuron* 102, 1127–1142.e3.

Flore, G., Cioffi, S., Bilio, M., and Illingworth, E. (2017). Cortical development requires mesodermal expression of Tbx1, a gene haploinsufficient in 22q11.2 deletion syndrome. *Cereb. Cortex* 27, 2210–2225.

Forneris, F., Binda, C., Vanoni, M. A., Mattevi, A., and Battaglioli, E. (2005). Histone demethylation catalysed by LSD1 is a flavin-dependent oxidative process. *FEBS Lett.* 579, 2203–2207. doi: 10.1016/j.febslet.2005.03.015

Fulcoli, F. G., Franzese, M., Liu, X., Zhang, Z., Angelini, C., and Baldini, A. (2016). Rebalancing gene haploinsufficiency in vivo by targeting chromatin. *Nat. Commun.* 7:11688.

Green, R., Allen, L. H., Bjørke-Monsen, A.-L., Brito, A., Guéant, J.-L., Miller, J. W., et al. (2017). Vitamin B12 deficiency. *Nat. Rev. Dis. Primer* 3:17040.

Haddad, R. A., Clines, G. A., and Wyckoff, J. A. (2019). A case report of T-box 1 mutation causing phenotypic features of chromosome 22q11.2 deletion syndrome. *Clin. Diabetes Endocrinol.* 5:13.

Hirsch, M. R., Tiveron, M. C., Guillemot, F., Brunet, J. F., and Goridis, C. (1998). Control of noradrenergic differentiation and Phox2a expression by MASH1 in the central and peripheral nervous system. *Dev. Camb. Engl.* 125, 599–608. doi: 10.1242/dev.125.4.599

Lania, G., Bresciani, A., Bisbocci, M., Francone, A., Colonna, V., Altamura, S., et al. (2016). Vitamin B12 ameliorates the phenotype of a mouse model of DiGeorge syndrome. *Hum. Mol. Genet.* 25, 4369–4375.

Lania, G., Zhang, Z., Huynh, T., Caprio, C., Moon, A. M., Vitelli, F., et al. (2009). Early thyroid development requires a Tbx1-Fgf8 pathway. *Dev. Biol.* 328, 109–117. doi: 10.1016/j.ydbio.2009.01.014

Lindsay, E. A., Vitelli, F., Su, H., Morishima, M., Huynh, T., Pramparo, T., et al. (2001). Tbx1 haploinsufficieny in the DiGeorge syndrome region causes aortic arch defects in mice. *Nature* 410, 97–101. doi: 10.1038/35065105

Motahari, Z., Moody, S. A., Maynard, T. M., and LaMantia, A.-S. (2019). In the line-up: deleted genes associated with DiGeorge/22q11.2 deletion syndrome: are they all suspects? *J. Neurodev. Disord.* 11:7.

Mukherjee, A., Carvalho, F., Eliez, S., and Caroni, P. (2019). Long-Lasting rescue of network and cognitive dysfunction in a genetic schizophrenia model. *Cell* 178, 1387–1402.e14.

Napoli, E., Tassone, F., Wong, S., Angkustsiri, K., Simon, T. J., Song, G., et al. (2015). Mitochondrial citrate transporter-dependent metabolic signature in the 22q11.2 Deletion Syndrome. *J. Biol. Chem.* 290, 23240–23253. doi: 10.1074/jbc.m115.672360

Nilsson, S. R. O., Heath, C. J., Takillah, S., Didienne, S., Fejgin, K., Nielsen, V., et al. (2018). Continuous performance test impairment in a 22q11.2 microdeletion mouse model: improvement by amphetamine. *Transl. Psychiatry* 8:247.

Ogata, T., Niihori, T., Tanaka, N., Kawai, M., Nagashima, T., Funayama, R., et al. (2014). TBX1 mutation identified by exome sequencing in a Japanese family with 22q11.2 deletion syndrome-like craniofacial features and hypocalcemia. *PloS One* 9:e91598. doi: 10.1371/journal.pone.0091598

Paxinos, G., and Franklin, K. (2012). *Mouse Brain in Stereotaxic Coordinates.* New York, NY: Academic Press.

Paylor, R., Glaser, B., Mupo, A., Ataliotis, P., Spencer, C., Sobotka, A., et al. (2006). Tbx1 haploinsufficiency is linked to behavioral disorders in mice and humans: implications for 22q11 deletion syndrome. *Proc. Natl. Acad. Sci. U S A.* 103, 7729–7734. doi: 10.1073/pnas.0600206103

Paylor, R., and Lindsay, E. (2006). Mouse models of 22q11 deletion syndrome. *Biol. Psychiatry* 59, 1172–1179. doi: 10.1016/j.biopsych.2006.01.018

Prasad, S. E., Howley, S., and Murphy, K. C. (2008). Candidate genes and the behavioral phenotype in 22q11.2 deletion syndrome. *Dev. Disabil. Res. Rev.* 14, 26–34. doi: 10.1002/ddrr.5

Racedo, S. E., Hasten, E., Lin, M., Devakanmalai, G. S., Guo, T., Ozbudak, E. M., et al. (2017). Reduced dosage of β-catenin provides significant rescue of cardiac outflow tract anomalies in a Tbx1 conditional null mouse model of 22q11.2 deletion syndrome. *PLoS Genet.* 13:e1006687. doi: 10.1371/journal.pgen.1006687

Shi, Y., Lan, F., Matson, C., Mulligan, P., Whetstine, J. R., Cole, P. A., et al. (2004). Histone demethylation mediated by the nuclear amine oxidase homolog LSD1. *Cell* 119, 941–953.

Tamura, M., Mukai, J., Gordon, J. A., and Gogos, J. A. (2016). Developmental inhibition of Gsk3 rescues behavioral and neurophysiological deficits in a mouse model of schizophrenia predisposition. *Neuron* 89, 1100–1109. doi: 10.1016/j.neuron.2016.01.025

Torres-Juan, L., Rosell, J., Morla, M., Vidal-Pou, C., García-Algas, F., de la Fuente, M.-A., et al. (2007). Mutations in TBX1 genocopy the 22q11.2 deletion and duplication syndromes: a new susceptibility factor for mental retardation. *Eur. J. Hum. Genet. EJHG* 15, 658–663. doi: 10.1038/sj.ejhg.5201819

Vitelli, F., Lania, G., Huynh, T., and Baldini, A. (2010). Partial rescue of the Tbx1 mutant heart phenotype by Fgf8: genetic evidence of impaired tissue response to Fgf8. *J. Mol. Cell Cardiol.* 49, 836–840. doi: 10.1016/j.yjmcc.2010.08.023

Xu, H., Chen, L., and Baldini, A. (2007). In vivo genetic ablation of the periotic mesoderm affects cell proliferation survival and differentiation in the cochlea. *Dev. Biol.* 310, 329–340. doi: 10.1016/j.ydbio.2007.08.006

Xu, H., Morishima, M., Wylie, J. N., Schwartz, R. J., Bruneau, B. G., Lindsay, E. A., et al. (2004). Tbx1 has a dual role in the morphogenesis of the cardiac outflow tract. *Dev. Camb. Engl.* 131, 3217–3227. doi: 10.1242/dev.01174

Zhang, Z., Cerrato, F., Xu, H., Vitelli, F., Morishima, M., Vincentz, J., et al. (2005). Tbx1 expression in pharyngeal epithelia is necessary for pharyngeal arch artery development. *Dev. Camb. Engl.* 132, 5307–5315. doi: 10.1242/dev.02086

Conflict of Interest: The authors declare that the research was conducted in the absence of any commercial or financial relationships that could be construed as a potential conflict of interest.

Publisher's Note: All claims expressed in this article are solely those of the authors and do not necessarily represent those of their affiliated organizations, or those of the publisher, the editors and the reviewers. Any product that may be evaluated in this article, or claim that may be made by its manufacturer, is not guaranteed or endorsed by the publisher.